Journal of Hydrology 621 (2023) 129643

Contents lists available at ScienceDirect

Journal of Hydrology

journal homepage: www.elsevier.com/locate/jhydrol

Research papers

Towards a better understanding of time-lags in karst aquifers by combining hydrological analysis tools and dye tracer tests. Application to a binary karst aquifer in southern Spain

J.F. Martín-Rodríguez *, M. Mudarra, B. De la Torre, B. Andreo

Centre of Hydrogeology of the University of Málaga (CEHIUMA), Edificio I+D Ada Byron, C/ Arquitecto Francisco de Peñalosa 18. 29071, Málaga, Spain

ARTICLE INFO

Keywords:
Carbonate (karst) aquifer
Time-lag
Recharge
Dye tracer test
Cross correlation function
Southern Spain

ABSTRACT

The assessment of the response time of a karst aquifer is an important step towards the development of conceptual models from which tools for water resources planning and management could be applied. The aim of this work is to evaluate the applicability of the joint use of statistical time-lag evaluation and dye tracer tests techniques with a double objective: 1) the development of conceptual models on the hydrogeological functioning that include the duality in the aquifer recharge processes, as well as the particularities of the preferential drainage flowpaths respect to the global response of the aquifers; 2) to establish a reference frame to foresee with enough time in anticipation the potential affections derived from the concentrated recharge to the springs, required in the creation of water quality monitoring networks and early warning systems to water pollution. In the Ubrique karst aquifer (southern Spain), the empirical relationships between the intensity (I) of rainfall events (recharge) and the time-lag (T) observed in the springs that draining the aquifer have been quantified. The establishment of the curve (I-T) constitutes a reliable tool for the prediction of potential affections to the springs (intended for urban supply) derived from recharge events. On the other hand, the comparison of the values drawn in the I-T curve, characteristic of each spring, with those derived from three tracer tests, has allowed further advances in the understanding of the aquifer functioning and the influence of concentrated recharge on the global system behavior to be achieved.

1. Introduction

Carbonate massifs are particularly susceptible to fracturing and karstification phenomena, forming complex aquifer systems in which the infiltration of water occurs through stratification surfaces, discontinuities, and/or fissures enlarged by dissolution, and within the rock matrix. This set of elements generally constitutes a hierarchical drainage network, capable of rapidly transmitting large volumes of water from infiltration zones (recharge areas) to natural drainage points (generally springs). There are several factors that control recharge in these systems: climatic conditions, lithology and degree of karstification, topographic position, soil surface components (vegetation, texture, porosity, fractures, etc.), slope and soil moisture (Andreo et al., 2008; Fu et al., 2015; Galibert, 2016).

In addition, tectonics is a factor that increases the complexity of aquifer systems, often being a critical element affecting hydrogeological behaviour, particularly in mountainous regions (Goldscheider, 2005; Perrin and Luetscher, 2008; Sanz de Galdeano et al., 2019; De la Torre et al., 2020). Due to these factors, karst aquifers present a high degree of heterogeneity (spatial anisotropy) in their hydrogeological properties (Bakalowicz, 2005; Ford and Williams, 2007; Worthington and Ford, 2009), being also much more vulnerable to contamination than other systems (Doerfliger and Zwahlen 1998; Marín and Andreo, 2015; Marín et al., 2021, Hartmann et al., 2021). It is essential therefore to highlight the strategic dimension of carbonate aquifers, and to manage the foreseeable water scarcity crisis induced by global climate change (Konapala et al., 2020), since around 25% of the world's population supplies its demands with water from this type of aquifers (EU, 1995; Ford and Williams, 2007; Stevanović, 2018).

The implementation and contrast of several research methodologies provide a consistent framework to improve knowledge about karst aquifer functioning, including aspects related to recharge mechanisms (Trček, 2007; Charlier et al., 2012), surface water-groundwater relationship (Bailly-Comte et al., 2009), transport dynamics towards

* Corresponding author.
E-mail address: josefranciscomr@uma.es (J.F. Martín-Rodríguez).

https://doi.org/10.1016/j.jhydrol.2023.129643
Received 21 February 2023; Received in revised form 19 April 2023; Accepted 9 May 2023
Available online 13 May 2023
0022-1694/© 2023 The Author(s). Published by Elsevier B.V. This is an open access article under the CC BY-NC-ND license (http://creativecommons.org/licenses/by-nc-nd/4.0/).

preferential drainage routes (Schuler et al., 2020), groundwater flow and storage at different aquifer components (Perrin et al., 2003), or internal aquifer geometry (Bodin et al., 2022), among others. Hydrological methods (water balance, hydrodynamic analyses, etc.) deserve special attention since they have demonstrated applicability to elucidate conceptual schemes of functioning in geologically complex contexts (Padilla and Pulido-Bosch, 1995; Groves et al., 2007; El-Hakim and Bakalowicz, 2007; De la Torre et al., 2020). In this sense, some authors (Jiang et al., 2008; Galibert, 2016) discussed the close relationship between the precipitation intensity (considering effective rainfall as the primary factor controlling the aquifer recharge) and the time-lag until input detection at shallow subsurface observation points. Based on Mangin's correlation analysis (1981), Delbart et al. (2014) extend this relationship by studying the temporal variability of water transfer through the infiltration zone of karst aquifers, using the Sliding Window Cross Correlation Function (SWCCF) to estimate the time-lag between rainfall and the piezometric level time series in wells and boreholes as indicators of the recharge effects. It should be noted that the hydrodynamic conditions of the aquifer prior to a recharge event can modify the responses (hydrochemical and hydrodynamic) that are recorded at the discharge points (Perrin et al., 2003; Bicalho et al., 2012; Fu et al., 2015).

The application of Delbart et al. (2014) approach to the entire aquifer, considering natural discharge points (springs) as the reference of the hydrodynamic response, has the advantage of achieving a global assessment of the aquifer functioning. Moreover, the use of precipitation (the driving cause of the system response) as a temporal reference for evaluating the impacts of quick recharge events on springs shows relevant benefits, since rainfall records are usually real time available and provide a wider temporal range than indicators based on intrinsic water parameters, whose detection is an immediate indication of water pollution. Hence, it is expected that the empirical relationship between the input signal and its hydraulic effects in the outlets (rainfall intensity -I- versus response lag-time -T-; "I-T curve" in this document) provide a quantitative predictive tool for assessing the impact of recharge processes on discharge points, especially valuable when these are intended for human supply.

The joint use of the I-T curves, characteristic of the global system response, with results derived from dye tracer tests, whose usefulness in karst hydrogeology is well known (Benischke et al., 2007; Goldscheider et al., 2008), adds the perspective of the time-lags along defined drainage flow paths (commonly between concentrated infiltration points and springs). Consequently, the combination of both methods under the same approach would open new insights for inferring the presence and influence of geometric constraints that may exert a noteworthy incidence on the velocity of input signal transmission into the aquifer. The main aim of this work is, therefore, to advance on the understanding of the factors that drive the hydrodynamic time-lag in binary karst aquifers under different hydrometeorological conditions affecting recharge volume. In addition, we try to explore the potential of the joint application of hydrological analysis tools and dye tracer tests to gain a deeper insight on the mechanisms that modulate the response of these aquifers to recharge processes.

With an integral view, both temporal and spatial, the approach presented here could help in management strategies, with special relevance to those oriented to protect the water supply sources in karst aquifers. In fact, the test site where our approach is applied (Sierra de Ubrique, S Spain) acts as pilot area for the development of early warning systems (EWS) to avoid the water pollution during flooding events (Marín et al., 2021; Martín-Rodríguez et al., 2022). The establishment of the lag-time of the point draining the system and used as sources of urban water supply may constitute the necessary conceptual framework for the implementation of control algorithms and to enhance their predictability when faced with increasingly changing and extreme hydroclimatic scenarios (Richts and Vrba, 2017).

1.1. Site settings

The Ubrique aquifer is a binary karst system located at NE area of the Cádiz province, southern Spain (Fig. 1), with a total surface -effective recharge area- of 26.06 km^2. The karst system is formed by two mountainous massifs (Caíllo and Ubrique sierras) with a ragged orography (from 317 to 1395 m a.s.l.), dominated by outcrops of carbonate rocks (Jurassic dolostones and limestones). The prevailing climate in the area is humid Mediterranean, with a noteworthy seasonal pattern in the annual distribution of precipitation and air temperature. Rainfall mainly occurs from autumn to springtime, related to wet winds coming from the Atlantic Ocean. The mean annual precipitation and air temperature values recorded in this area (from 1984/85 to 2017/18) were respectively 1305 mm and 14.8 °C. Spatial distributions of both precipitation and temperature values are mostly conditioned by the altitude and the orientation of major hillsides. The accumulated rainfall amount for each hydrological year comprising the study period considered in this work (from October 2013 to September 2018) was respectively: 1,348 mm (2013/2014), 1,071 mm (2014/2015), 1,208 mm (2015/2016), 807 mm (2016/2017) and 1,710 mm (2017/2018) (Table 1). The annual rainfall values were obtained through the spatial distribution of the isohyets lines for each hydrological year. Despite of rainfall amounts, several townships in the region dependent of groundwater resources for water supply are affected by seasonal restrictions.

Geologically, the pilot site and surrounding areas are located within the westernmost sector of the Betic Cordillera, specifically within the so-called Penibetic Domain of the External Zone (Martín-Algarra, 1987). The stratigraphic series of this domain consists of around 500 m thick Jurassic dolostones and limestones, which present Late Triassic clays, dolomitic beds, sandstones, and evaporite rocks (mainly gypsum) at the bottom, and Early Cretaceous-Tertiary marly-limestones and marls at the top. Surrounding and overlaying all these rocks, Tertiary Flysch-type clays and sandstones outcrops (Figs. 1 and 2). The geological structure is characterized by NE-SW pluri-kilometer-size open anticline folds and narrow synclines, affected by reverse faults from which overthrusts were developed with vergence towards N-NW. Tectonic gave rise to a series of imbricate thrusts, with the Triassic rocks overthrusting Cretaceous marls under Jurassic carbonate formations (cross-section 1-1́ in Fig. 2). Apart from these shortening features, the entire structure has been affected by normal faults, in a mainly NNE – SSW direction, and oblique strike-slip fractures, caused by extensional accommodation of prior structures (Jiménez-Bonilla et al., 2017). The SW border of the Sierra de Ubrique has been also affected by a more recent set of normal faults (related to gravitational collapses), which configure the orography in that sector (cross-section 2-2́).

The large outcrops of Jurassic limestones, densely fractured, jointly with bedding planes and the prevailing climate conditions, have favored a noteworthy development of exokarst landforms (Delannoy, 1987; 1999): karrenfields, dolines, sinkholes, and shafts. Besides, the presence of low-permeability outcrops (marls and clays) related to synclinal folds and faults have contributed to the development of endorheic drainage areas, which caused the quick infiltration of runoff water generated during rainfall events through several swallow holes hydrologically connected with shafts and other endokarst features. In general, a patchy soil cover up to 10–20 cm thick can be found, especially where the slope is low. Overall vegetation is typically Mediterranean with shrub growth forest and pasture, except for the highest areas, where there is neither soil development nor vegetation. In these areas, large karrenfields exist over bare carbonate rocks.

In hydrogeological terms, the Ubrique karst system is formed by fractured and karstified Jurassic carbonate rocks, limited by low permeability materials (Cretaceous-Tertiary marls, Triassic clays, and Flysch clays) in almost all their borders (Figs. 1 and 2). The geometry of the aquifer is particularly determined by the flat-hinge anticline structure and occasionally by low permeability materials imbricates below the thrust surfaces (Andreo et al., 2014). Recharge takes place by two

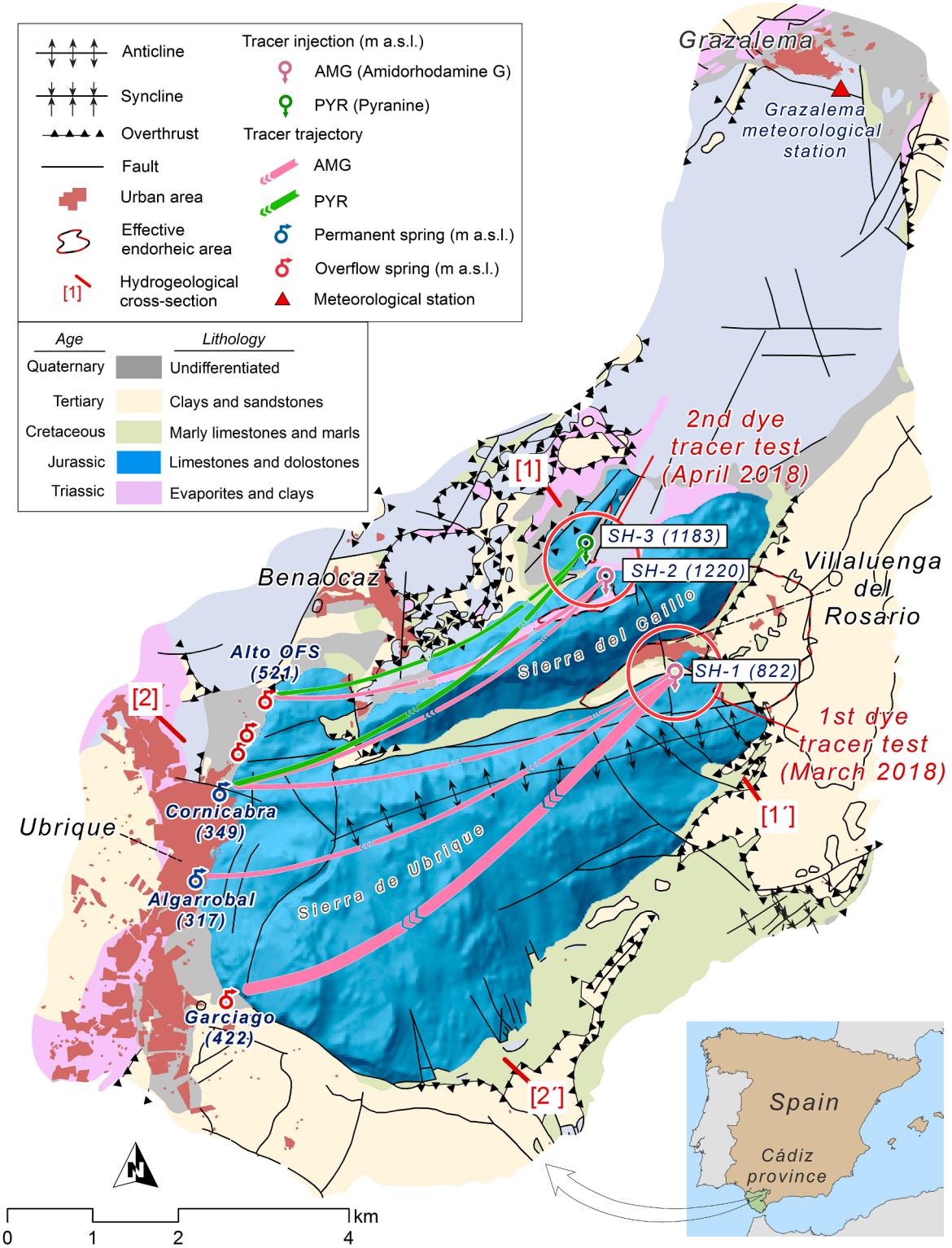

Fig. 1. Location of the study site and geological and hydrogeological features of the Ubrique karst system. The situation of 1 – 1́ and 2 – 2́ cross-sections of Fig. 2 is also shown.

mechanisms (binary karst system): by direct infiltration of rainwater over the bare carbonate outcrops (autogenic component, 24.03 km^2) and by concentrated infiltration of runoff water coming from small neighbor catchments formed by low-permeability materials (allogenic component, 2.03 km^2). The hydrogeological connection of three of the swallow holes (SH-1, SH-2, and SH-3 in Fig. 1) with some of the springs was proved using dye tracers. Hydrogeochemical tools applied to this site also revealed the existence of an incipient degree of contamination affecting the system as a whole (Marín et al., 2021), whose origin would be associated with the infiltration of surface runoff water through the Villaluenga del Rosario shaft (SH-1 in Fig. 1). This point receives the poorly treated wastewater from 500 inhabitants (urban area of Villaluenga del Rosario) as well as the remains of the livestock activity over an endorheic area of 2.03 km^2 (Fig. 1). Groundwater discharge occurs

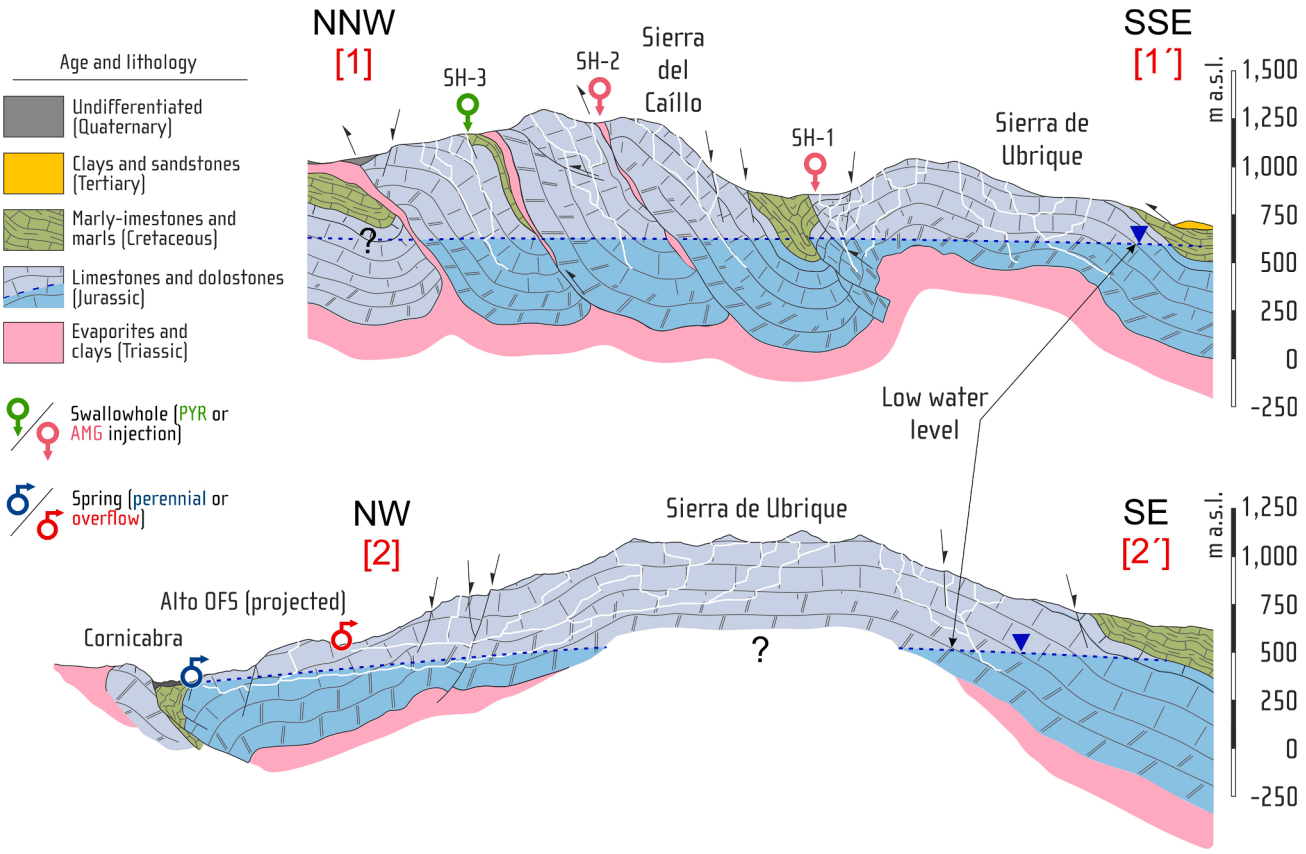

Fig. 2. Geological – hydrogeological cross-sections of the Ubrique karst system, showing the geometry of the aquifer. See location in Fig. 1.

along the W border of the carbonate outcrops, through two perennial springs sited at the Ubrique urban area (Cornicabra and Algarrobal springs, located at 349 and 317 m a.s.l., respectively), plus two overflow springs: one located north of Ubrique town (Alto OFS, 521 m a.s.l.) and other one sited at the SW border of the Sierra de Ubrique (Garciago, 422 m a.s.l.). General background information about the hydrogeological settings of the pilot site can be found in previous works (Sánchez et al., 2016; Sánchez et al., 2018; Marín et al., 2021; Martín-Rodríguez et al., 2022).

2. Material and methods

2.1. Data availability and hydrodynamic analyses

Continuous discharge data from Cornicabra and Algarrobal permanent outlets, and also from Garciago overflow spring was hourly recorded during five hydrological years by using ODYSSEY^{TM} capacitance water level loggers, properly gauged with its corresponding rating curve, obtained through direct flow determinations by means OTT^{TM} C2 and ETRELEC^{TM} SALINOMADD flowmeters. Temperature and electrical conductivity –EC- of groundwater drained by the springs were also hourly monitored using different types of proves: ONSET^{TM} HOBO -U24-001- datalogger installed at Algarrobal spring, and WTW^{TM} Cond 3310 at Cornicabra outlet. Precipitation data were hourly obtained from a rain gauge station located near Grazalema town (red triangle in Fig. 1).

During the monitoring period (2013/14–2017/18) the time-lag between the occurrence of rainfall events triggering the aquifer recharge and its manifestation in discharge rate risings of the springs has been measured (single time-lag determinations, STD). The time lag between the mass center of a single rainfall event (point when the 50% of the total precipitation is amounted) and the maximum flow rate value of the spring has been considered as the system response time to a specific recharge event (Fig. 3B). Several descriptors concerning to the precipitation events as, mean and maximum intensity, total rainfall amount and duration event have been estimated, in order to establish relationships among rainfall typology and springs time-lags.

On the other hand, cross-correlation analysis (CCF) has been performed for individual hydrological year using rainfall data series as input (hourly records recorded at Grazalema meteorological station -see location in Fig. 1-) and hourly data of discharge from each spring as output. The *k* values (that shows the mean time-lag between the impulse and the observed response in CCF analysis) obtained have been considered an annual mean time-lag (hours) for the hydrodynamic response of the system to precipitation events (Table 1). Commonly, higher values of time-lag are related to poorly developed karst drainage network and larger capacity to modulate the recharge impulse. Instead, short time lags illustrate a high capability of the karst system to transfer infiltration water from recharge areas to the outflow points (Mangin, 1984; Padilla and Pulido-Bosch, 1995; Fiorillo and Doglioni, 2010; Lorette et al., 2018).

The sliding window cross-correlation function analysis (SWCCF) consists of sectioning the precipitation and spring discharge time series into short and partially overlapping time periods (Fig. 3A). For each of these periods (observation windows) the cross-correlation function is calculated and the value of *k* is determined, thus obtaining a time-lag temporal distribution. This methodology allows to obtain the temporal evolution of the time lag among the input signal (precipitation data) and its response at the discharge points (spring discharge). A time length of the observation window of 60 days with a 50% overlap (30 days) has been here used (Fig. 3A), in order to reach the optimal resolution during the wet periods (commonly between autumn, winter and spring seasons). This methodology allows the evaluation of response times for specific periods, leading to the detection of seasonal patterns or highlighting differences between successive recharge episodes (Delbart et al., 2014).

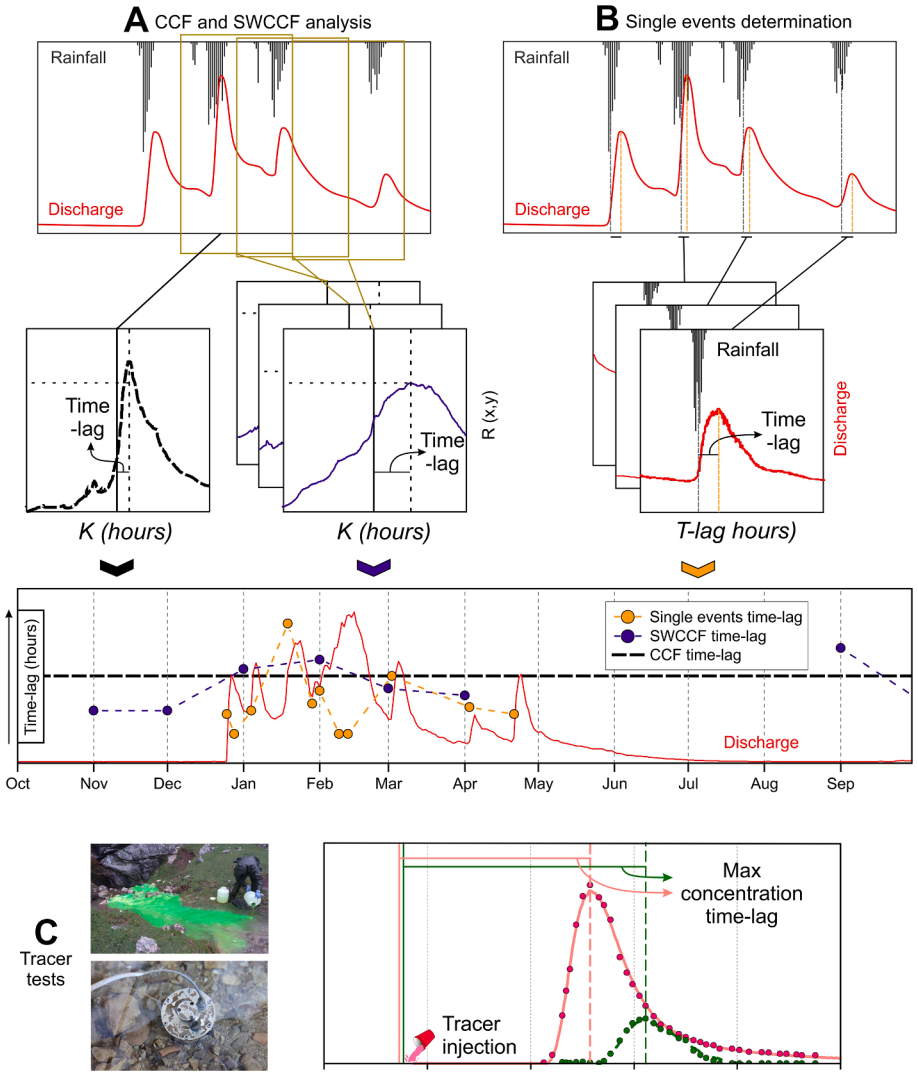

Fig. 3. Schematic representation of the workflow addressed in this research, including the parameter estimation routine to obtain the response times (in hours).

2.2. Dye tracer tests

Two dye tracer experiments were performed in the framework of this research using twice fluorescent substances (Table 1; Fig. 2): pyranine (PYR, solvent green 7; CAS 6358–69-6) and amidorhodamine G (AMG, Acid red 50, CAS: 5873–16-5). The first experiment was performed by injection of 3 kg of AMG into the Villaluenga del Rosario swallowhole (SH-1) on 07 March 2018, coinciding with a rainfall event of 157 mm of total amount, and a mean intensity rainfall value of 5.1 mm·h^{-1}. In response to this test, dye was detected in the three springs related to the drainage of the Ubrique aquifer: Cornicabra, Algarrobal, and Garciago.

The second test consisted of the near-simultaneous injection of two tracers (AMG, 3 kg, and PYR, 2 kg) on April 12th, 2018, in two karst swallowholes (SH-2 and SH-3, respectively) placed in the Sierra del Caillo (Fig. 1), and coinciding with a rainfall event of 53 mm. In this case, both tracers were detected in Cornicabra and Alto OFS springs. Groundwater sampling was performed manually, directly at the karst springs, with a sampling frequency between 1 and 5 h or, automatically, using a GGUN-FL30 portable fluorometer (Fig. 3C), whose reading frequency was 15 min. A Perkin-Elmer LS55 spectrofluorometer was used for the detection and quantitative determination (in the laboratory of the Center of Hydrogeology of the University of Málaga) of dye tracer concentration in spring water.

3. Results

3.1. Time-lag evaluation from hydrodynamic analysis tools: CCF, SWCCF and single determinations

The parameters concerning the main springs discharge regime are summarized in Table 1. In general terms, the three control points show a marked variability in their discharge flow rates, with minimum values not higher than 35 l·s^{-1} at the end of the hydrological year, which contrasts with the maximum values reached: 2623, 2694, and 10093 l·s^{-1} for Cornicabra, Algarrobal, and Garciago, respectively). Cornicabra spring shows the highest average flow rate (324 l·s^{-1}), in contrast to the mean value recorded in Algarrobal and Garciago springs (125 and 147 l·s^{-1}, respectively). Fig. 4 shows the hydrodynamic responses of the three main springs draining the pilot site, jointly with the hourly records of rainfall occurred during the study period. In contrast to the Cornicabra spring, in which each significant rainfall event induces a response, the hydrograph analysis of Algarrobal and Garciago reveals that not all rainfall impulses provoke an increase in discharge rates. This phenomena has been observed several times along the study period and it would be related to the previous hydrological conditions and the extent of drought periods (such as the first flooding events of the hydrological years 2015/16 and 2017/18), although in some cases it occurred in winter or spring time, as the year 2013/14 (Fig. 4). The *k* values

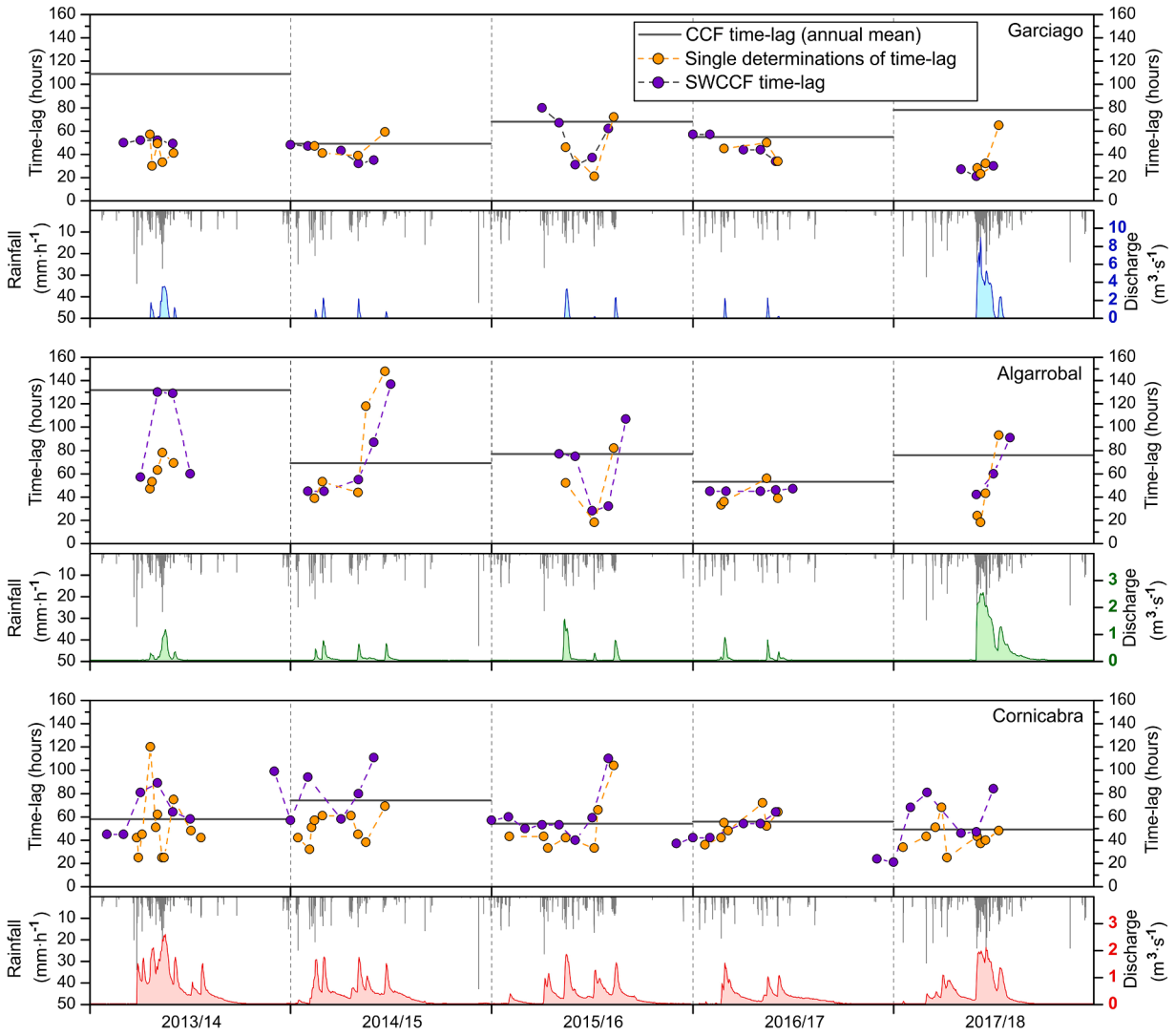

Fig. 4. Temporal distribution of springs response times, obtained from CCF, SWCCF and single determinations analysis, during the control period.

obtained both for each spring and for each hydrological year have been considered the mean annual response time or time-lag (hours). According to the results of the CCF response times (Table 1 and Fig. 5), the aquifer sector drained by Cornicabra, Algarrobal, and Garciago springs show rapid responses to rainfall events (58 to 81 h). These values have markedly ranged from a minimum of 49 h (obtained for the hydrological years 2017/18 -Cornicabra- and 2014/15 -Garciago-) to 132 h for a maximum value calculated in Algarrobal spring during the year 2013/

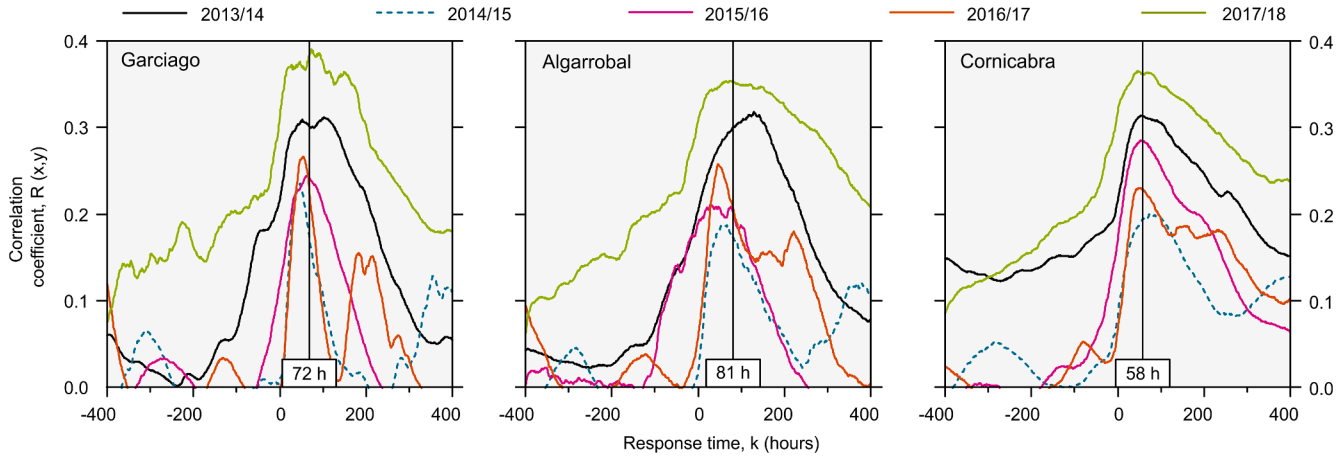

Fig. 5. Cross-correlation function (CCF) between rainfall and spring discharge (hourly data) and calculated mean response times, for each year of the study period.

Table 1
Summary of results obtained through CCF, SWCCF and single events determinations. **k**, value of lag between rainfall and spring discharge, determined through Cross-Correlation Function. **n***, number of periods with significant correlation coefficient for the SWCCF analysis. **n****, number of single recharge events identified for each hydrological year. **R**, Pearsons correlation coefficient.

			Discharge			CCF analysis		SWCCF analysis			Single events time-lag		
		Rainfall amount	*max value*	*mean value*	*min value*	*k value*	*R value*	*n**	*Mean k value*	*Mean R value*	*n***	*Rainfall intensity*	*Mean T-lag*
	Year	*(mm/year)*		*($l{\cdot}s^{-1}$)*		*(h)*	*(x,y)*		*(h)*	*(x,y)*		*($mm{\cdot}h^{-1}$)*	*(h)*
Cornicabra	*2013–2014*	1348	2623	435	23	58	0.31	6	64	0.31	11	2.7	51
	2014–2015	1071	1856	332	24	74	0.20	6	83	0.20	9	2.5	51
	2015–2016	1208	1899	303	22	54	0.29	8	60	0.21	7	2.8	53
	2016–2017	807	1542	215	22	56	0.23	6	49	0.31	7	1.7	53
	2017–2018	1710	2177	335	22	49	0.37	7	53	0.26	9	3.2	43
	mean	*1229*	2019	324	23	*58*	*0.28*		*62*	*0.26*		*2.6*	*50*
Algarrobal	*2013–2014*	1348	1238	89	34	132	0.32	4	94	0.38	5	1.6	62
	2014–2015	1071	825	83	28	69	0.19	5	74	0.17	5	1.6	80
	2015–2016	1208	1652	93	34	77	0.21	5	64	0.26	3	4.0	51
	2016–2017	807	941	72	35	53	0.26	5	46	0.26	4	1.9	41
	2017–2018	1710	2694	289	32	76	0.36	3	70	0.38	4	2.9	45
	mean	*1229*	1470	125	33	*81*	*0.27*		*70*	*0.29*		*2.4*	*56*
Garciago	*2013–2014*	1348	3797	142	0	109	0.31	4	51	0.34	5	1.6	42
	2014–2015	1071	2496	49	0	49	0.23	5	41	0.28	4	1.8	47
	2015–2016	1208	3364	73	0	68	0.24	5	55	0.27	3	4.0	46
	2016–2017	807	2548	35	0	55	0.27	5	47	0.31	3	1.9	43
	2017–2018	1710	10,039	436	0	78	0.39	3	26	0.40	4	2.9	37
	mean	*1229*	4449	147	0	*72*	*0.29*		*44*	*0.32*		*2.4*	*43*

14.

The sliding window cross-correlation (SWCCF) method between precipitation and the available discharge data series (5 years) has been applied (Table 1 and Fig. 4). 77 correlograms were obtained with a confidence value of 95%, whose correlation coefficient R [x,y] is higher than the standard error (Mangin, 1981; Delbart et al., 2014). Likewise, 83 flooding events were identified from which the time-lag respect to recharge input could be quantified (Table 1). To perform calculations for rainfall-related parameters (mean intensity, duration, total amount, etc.), the precipitation event that causes the recharge impulse was previously delimited. In dry seasons, usually from May to October, the absence of rainfall and the weak variation in the discharge rate of the springs means that the results of the SWCCF analysis are not representative (no considered in this work).

As it is shown in Fig. 4 and Table 1, the response time estimated by SWCCF analysis and single determinations in each of the springs is far from being uniform throughout the year, as may be inferred from the CCF analysis suggest. A noteworthy variability in the response time values can be observed during the wet periods. For example, the annual mean response times in Cornicabra spring ranged between a maximum value of 83 h (result obtained during the year 2014/15 using the SWCCF analysis) and a minimum value of 43 h, measured in the recharge events of 2017/18 (single events time-lag determinations). In general terms, Algarrobal spring showed the greatest mean annual time-lag value, with a minimum of 41 h (single events time-lag), determined for the flooding events of 2016/17, and a maximum of 132 h during the year 2013/14 (CCF analysis). The mean value of the spring time-lag during the study period ranged between 56 h (single events determinations) and 81 (CCF results). Garciago overflow spring shows the shortest response times with an annual minimum value of 26 h during the year 2017/18 (SWCCF analysis tool). The maximum value was determined by CCF analysis during the year 2013/14 (109 h).

3.2. Dye tracer tests

During the first tracer test performed in the framework of this research (March 2018), the first detection time (T_{fd}) of the dye was verified in Cornicabra spring 31 h after infection (Fig. 6), followed by Garciago (45 h) and finally Algarrobal (47 h after injection). The time-lags for the maximum tracer concentration followed a similar pattern to that defined by the first detection times: 39 h in Cornicabra (maximum concentration of 0.20 μg/l), 55 h in Garciago (1.46 μg/l), and 64 h in Algarrobal (0.89 μg/l; Table 2). A temporal coincidence of the maximum tracer concentration and the relative minimum values of EC and T (Fig. 6) were detected in Cornicabra and Algarrobal springs. The breakthrough curves (i.e., BTCs) obtained at Algarrobal and Garciago springs show also a secondary peak of dye concentration, between 46 and 55 h after maximum concentration (Fig. 6). The recovery rate values at the end of the first experiment were 68.4% (Garciago), 21.9% (Algarrobal), and 2.03% (Cornicabra), with a total mass recovered during this experiment of 92.3%.

In the subsequent tracer test (April 2018), the injected dyes in SH-2 and SH-3 (see location in Fig. 1) were only detected in the water drained by Cornicabra spring and in its related set of overflow springs (Fig. 1), although samples were only systematically collected in Alto OFS (Fig. 7) due to better accessibility conditions. Despite the reduced time interval between the injections of both dyes and the similar distance from the SH-2 and SH-3 injection points to the springs (Table 2), the detection of AMG was substantially faster than PYR, both for the first detection and for the maximum concentration values (Fig. 7 and Table 2). T_{mc} and T_{fd} for AMG were respectively 34 and 44 h in Cornicabra spring, and 37 and 42 h for Alto OFS (Table 2). The highest concentration reached was quite comparable in both springs (12.95 and 10.62 $\mu g{\cdot}l^{-1}$). In the case of PYR, the first detection and maximum concentration times were higher than obtained for AMG, with 46 and 57 h in Cornicabra spring, and 48 and 56 h in Alto OFS, reaching peak concentrations 3.20 and 3.68 $ug{\cdot}l^{-1}$,

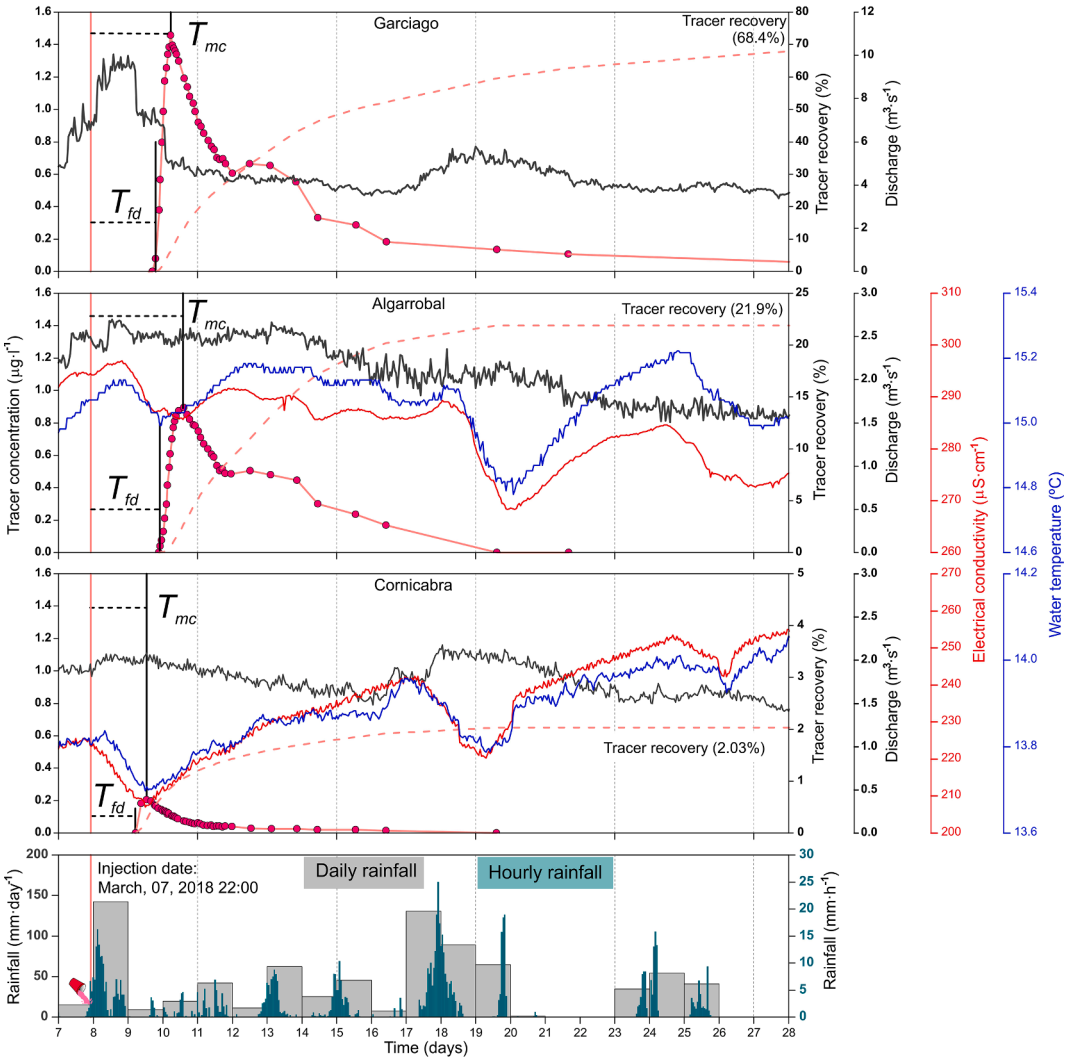

Fig. 6. Tracer breakthrough curves (BTĆs) of amidorhodamine G (AMG) in Cornicabra, Algarrobal and Garciago springs. Injection in SH-1 (see location in Fig. 1).

respectively. In this test, the dye tracer recovery rate could only be quantified from Cornicabra BTĆs, yielding 38.9% for AMG and 11.2% for PYR (Table 2). These values, which are low compared to the previous test, were probably motivated by the impossibility of determining the quantitative recovery in overflow springs that showed the presence of both tracers (as in the Alto OFS), due to the absence of discharge records.

4. Discussion

The joint analysis of the results derived from the hydrological series processing (global system response) and those from dye tracer tests (preferential flowpaths) has provided deeper insights into the flow dynamics within a karst system with confirmed duality in recharge mechanisms (autogenic and allogenic), and also under variable hydrometeorological conditions. Additionally, the combination of techniques used in this work has a great potential for assessing, from an integrated point of view, different aspects on the system response to rainfall intensity, as well as for increasing our understanding on the internal geometry of karst aquifers. In general, quick rises in flow rates after recharge events and shapes of BTC curves reveal the existence of a highly developed karst network in the pilot site, which permits fast flows and short transit times of groundwater within the system towards the springs, both from the soil and epikarst (diffuse recharge) and from specific points on the surface where concentrated infiltration occurs (e.g., swallow holes). However, a detailed review of the results obtained in the framework of this study allows distinguishing differences in the response times of the springs to recharge, both for the global response and from specific points, which can be attributed to spatial variations in the development of the karst drainage network.

4.1. Role of rainfall intensity in response lag-times of karst aquifers

Although the CCF analysis provides general information on the mean response time of aquifers to the input signal (Padilla et al., 1995; Panagopoulos and Lambrakis, 2006), its application loses reliability to identify changes in response times as a consequence of differences in the hydrodynamic conditions during recharge periods. This restriction has prompted the implementation of further statistical approaches such as Partial Correlation of Time Series (Jukić et al., 2011), Sliding Window Cross-Correlation Function -SWCCF- (Delbart et al., 2014) or Higher-Order Partial Correlation Function (Jukić et al., 2015), which bring additional information about the system response to recharge impulses in karst media. In this work, the correspondence of the time-lag data provided by the SWCCF analysis with the single determinations of time-lag (SDT) for each flooding event, supports the representativeness of this approximation as a descriptor of the specific response time interval for each karst spring. All applied analyses are referred to the fastest flow circulation of groundwater in natural regime; lower correlation peaks or/and long-term response associated with slower drainage mechanisms (fracture and fissure flow mechanisms domain) is beyond the scope of

Table 2
Summary of results obtained from the dye tracer tests performed in the test site of Ubrique aquifer.

1 st dye tracer test (March 2018)	Injection: AMG (SH-1)		Tracer	Mass	Date	Rainfall amount	mean intensity	Altitude				
				(kg)	07/03/2018	***(mm)***	***(mm·h^{-1})***	*m (a.s.l.)*				
			AMG	3	07/03/201822:00	157	5.1	822				
	Detection		First detection time-lag	Max conc. time-lag	Maximun concentration	Mean spring discharge*	Height gradient	Altitude	Distance to injection point	Max. Velocity	Modal Velocity	Tracer recovery
		Spring	***(h)***	***(h)***	***(μg·l^{-1})***	***(l·s^{-1})***		*m (a.s.l.)*	***(m)***	***(m·h^{-1})***	***(m·h^{-1})***	***(%)***
		Cornicabra	31	39	0.20	1869	0.086	349	5505	177.6	141.2	2.03
		OFS-1	—	—	—	—	—	—	—	—	—	—
		Algarrobal	47	64	0.89	2405	0.083	317	6104	129.9	95.4	21.94
		Garciago	45	55	1.46	5088	0.062	422	6492	144.3	118.0	68.41
2 nd dye tracer test (April 2018)	Injection: AMG (SH-2)		Tracer	Mass	Date	Rainfall amount	mean intensity	Altitude				
				(kg)	12/04/2018	***(mm)***	***(mm·h^{-1})***	*m (a.s.l.)*				
			AMG	3	12/04/201817:30	53	1.2	1220				
	Detection		First detection time-lag	Max conc. time-lag	Maximun concentration	Mean spring discharge*	Height gradient	Altitude	Distance to injection point	Max. Velocity	Modal Velocity	Tracer recovery
		Spring	***(h)***	***(h)***	***(μg·l^{-1})***	***(l·s^{-1})***		*m (a.s.l.)*	***(m)***	***(m·h^{-1})***	***(m·h^{-1})***	***(%)***
		Cornicabra	34	44	12.95	1277	0.170	349	5110	150.3	116.1	38.9
		OFS-1	37	42	10.62	—	0.170	521	4121	111.4	98.1	—
		Algarrobal	—	—	—	—	—	—	—	—	—	—
		Garciago	—	—	—	—	—	—	—	—	—	—
	Injection: PYR (SH-3)		Tracer	Mass	Date	Rainfall amount	mean intensity	Altitude				
				(kg)	12/04/2018	***(mm)***	***(mm·h^{-1})***	*m (a.s.l.)*				
			PYR	2	12/04/201818:25	53	1.2	1183				
	Detection		First detection time-lag	Max conc. time-lag	Maximun concentration	Mean spring discharge*	Height gradient	Altitude	Distance to injection point	Max. Velocity	Modal Velocity	Tracer recovery
		Spring	***(h)***	***(h)***	***(μg·l^{-1})***	***(l·s^{-1})***		*m (a.s.l.)*	***(m)***	***(m·h^{-1})***	***(m·h^{-1})***	***(%)***
		Cornicabra	46	57	3.20	1277	0.163	349	5128	111.5	90.0	11.2
		OFS-1	48	56	3.68	—	0.164	521	4037	84.1	72.1	—
		Algarrobal	—	—	—	—	—	—	—	—	—	—
		Garciago	—	—	—	—	—	—	—	—	—	—

this study.

Previous studies have highlighted the existence of seasonal patterns in the response time distribution, with the lowest time-lag coinciding with wet periods, due to a faster transference of input signal through a transmissive network of conduits and fissures when hydraulic head increases (Larocque et al., 1998; Lee et al., 2006; Mudarra et al., 2014). Other authors (Delbart et al., 2014, Sánchez et al., 2016) concluded that the variability in the intensity of rainfall events primarily contributes to the faster transmission of the input signal in karst systems. In our work, a minimum value around 20 h from the mass center of precipitations for the response time has been detected following the obtained I-T curves (Fig. 8). Delbart et al. (2014) regarded this limit as the maximum transfer velocity within the aquifer due to the saturation of the upper sector of the drainage network (unsaturated zone), in addition to the intrinsic system heterogeneity or karst anisotropy. However, the nature of the observation points in the aforementioned research (boreholes and wells) restricted the representativeness of their results to a limited segment of the drainage network.

In contrast to Delbart et al. (2014), our study is exemplified in a mountainous karst aquifer characterized by a well-defined recharge area, a clear duality in recharge modalities, and a dataset coming from the main springs (Fig. 1). The most significant advantage of considering the hydrodynamic regime of the springs as a reference for response is to obtain a global view of the aquifer behavior, not restricted to a specific sector or subsystem within it. In all the analyzed springs, the lower asymptotic segment of the I-T curve (Fig. 8) represents the maximum flow transmission velocity under intense rainfall conditions, which in turn is indicative of the existence of a well-hierarchized karst network with high capacity to evacuate rapidly recent infiltrated water (Fig. 9). Nevertheless, while Algarrobal and Garciago springs shows a stabilization of the response time around 20 h (Fig. 8B and C), the minimum value reaches in Cornicabra outlet was around 30 h (Fig. 8A). At these conditions, when the first tracer test was carried out, karst conduits and enlarged fractures that feed Algarrobal and Garciago outlets would have a higher groundwater flow transmission capacity, compared to the sector drained by Cornicabra spring. This would be in agreement with the mean discharge rates shown by the two first outlets (Table 1) and also since both springs gathered the most of the injected dye mass in SH-

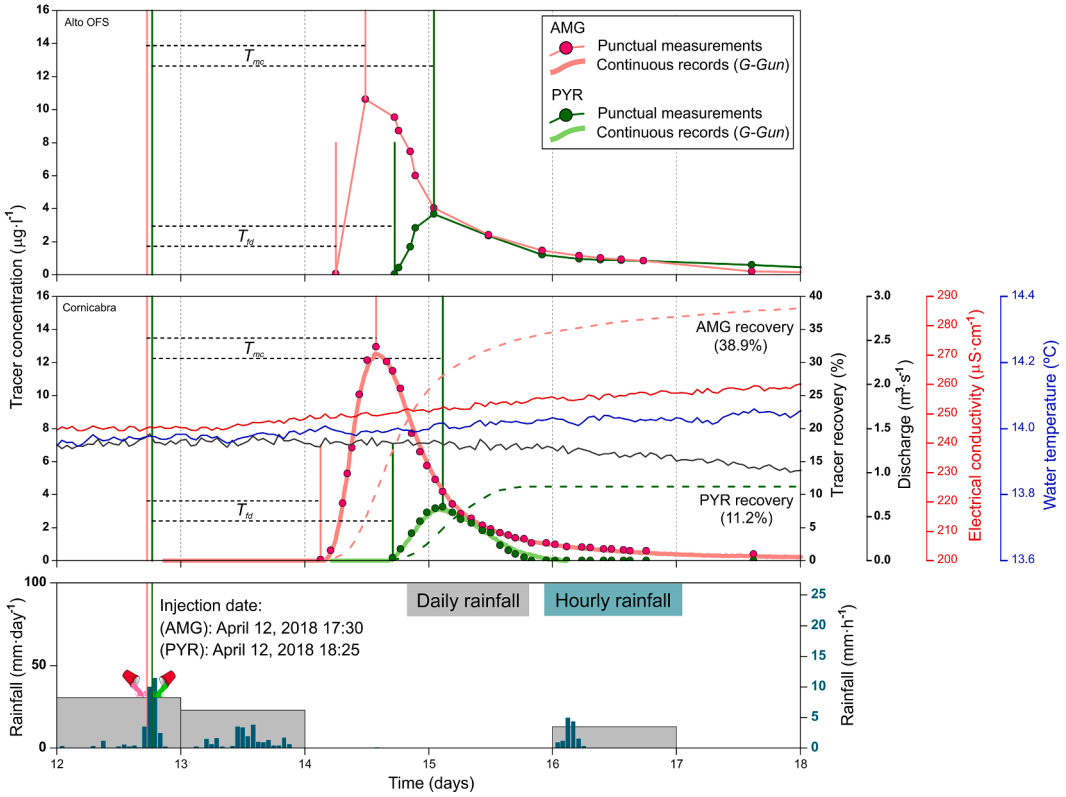

Fig. 7. Tracer breakthrough curves (BTCs) of amidorhodamine G (AMG) and pyranine (PYR) in Cornicabra spring and Alto OFS. Injection in SH-2 and SH-3, respectively (see location in Fig. 1).

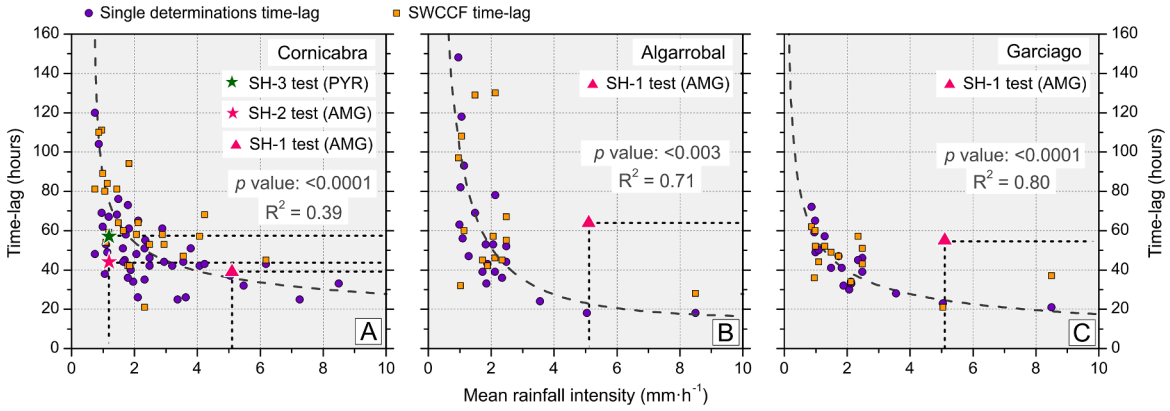

Fig. 8. Rainfall intensity versus response time inferred from SWCCF and single time-lag determination (I-T curve) for each studied spring draining the Ubrique aquifer. Time-lags of maximum concentration obtained through several dye tracer test is also shown.

1 (68.41% and 21.94%, respectively; Table 2). However, since the T_{mc} values calculated in Algarrobal and Garciago springs were significantly higher than expected, according to their experimental I-T curves (Fig. 8B and C), some type of geometric features capable to delay the arrival to the springs of the allogenic recharge from SH-1 must be invoked (Fig. 9).

The structure of the drainage network in several levels where karstification is differentially developed could lead to the existence of thresholds that require a certain rise in the hydraulic load to activate groundwater drainage. This scenario, illustrated on the left side of Fig. 9, implies an increase in the tortuosity of a specific drainage route, showing this higher transit time respect to the global time-lag of the system consequently. This functional scheme is consistent with the hydrodynamic regime of the Graciago and Algarrobal springs: while the first outlet is only activated after the most intense recharge events, the second one is limited to show notable increases in discharge flow in response to the most significant recharge events, although it drains a very low permanent flow (30–50 $l \cdot s^{-1}$).

By contrast, Cornicabra spring displayed a limited connection with SH-1 (tracer recovery ~ 2%), being a marginal drainage pathway under the same hydrometeorological conditions (Fig. 9). However, the satisfactory fit of the dye T_{mc} values on the I-T curve (Fig. 8A) suggests that the concentrated recharge is incorporated into a well-hierarchised drainage network in which water from both rapid infiltration through swallowholes and diffuse infiltration flows to the discharge points (Cornicabra and OFS). In addition, the maximum concentration of tracer occurred coinciding upon a relative minimum of EC and water temperature values in this outlet (Fig. 6). All this implies that the impact of the concentrated recharge mechanisms on the spring water is

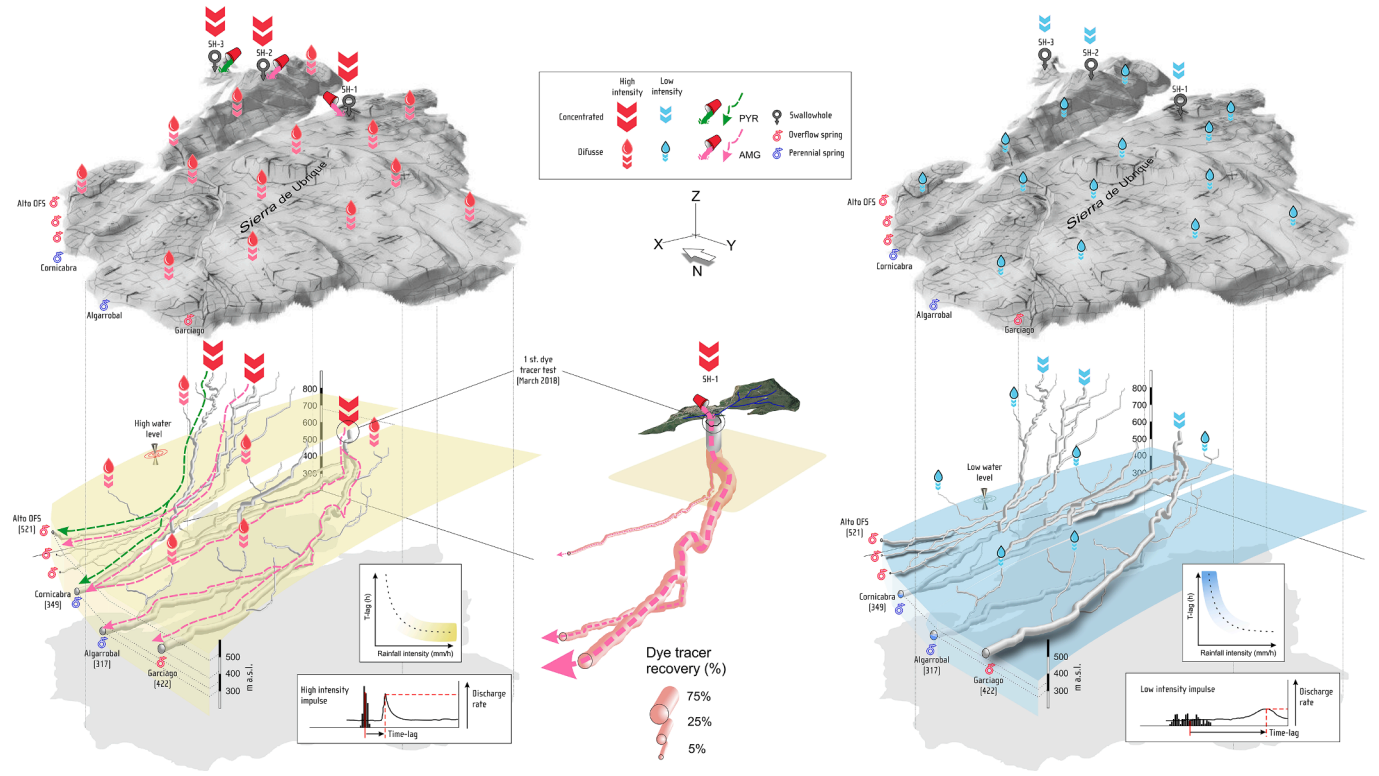

Fig. 9. Conceptual scheme of the hydrodynamic functioning of the Ubrique aquifer under two different hydrometeorological scenarios: high recharge intensity (left) and moderate-low recharge intensity (right). Flow dynamic within the karst system with confirmed duality in recharge mechanisms (autogenic and allogenic) after dye tracer experiments is also shown. Joint analysis of global and punctual responses of the karst system. Implications for aquifer management.

simultaneously manifested with the global response in the discharge peaks. At any case, a total recovery rate around 90% of the initially injected mass suggests no significant loss of dye through unmonitored drainage points, adsorption phenomena, or long-term storage (Käss, 1998).

On the other hand, global time lag values higher than 40–50 h (upper asymptotic section of the I-T curve, Fig. 8) are related to recharge events induced by rainfall of moderate-small intensities (Fig. 9, right side). Under these conditions, concentrated recharge may be marginal respect to diffuse recharge because the required conditions for the runoff generation over the catchment basins linked to karst swallow-holes not occur. Thus, rainwater diffusely infiltrated on permeable outcrops plays a predominant role in the global system response. The interaction with soil, epikarst and the unsaturated zone of the aquifer buffers the transmission rate of the input signal through the critical zone of the aquifer and may even act as a significant storage element in karst systems (Perrin et al., 2003).

Therefore, the magnitude of the recharge episodes could be not enough to provoke a significant rise in the hydraulic gradient and, consequently, groundwater flows occur predominantly through fractures/fissures. However, a part of recent infiltrated water could be transferred through a network of transmissive karst conduits according to the general morphology of the spring hydrographs, and also to the acceptable fitting of the T_{mc} values in the I-C curve achieved in Cornicabra outlet during the second tracer test (Fig. 8A). Although dyes were injected almost simultaneously (Table 2), at the same altitude (gradient), and at a similar distance to the spring, the T_{mc} value related to the PYR injected in SH-3 showed a better fit to the I-T curve. This fact could be due to a more efficient capacity of groundwater transference between SH-2 and the discharge points, which would be linked to preferential flows in the NE–SW direction, according to the main fold axis and fractures network of the pilot site (Fig. 1). This would be in agreement with the maximum concentration values of BTCs and also with the recovery rate of the injected mass of each dye (38.9% for AMG and 11.2% for PYR; Fig. 7). Therefore, in contrast to the previous information deduced for Garciago and Algarrobal, the jointly analysis of dye tracer test results and the global hydrodynamic response of the Cornicabra spring allows to deduce the existence of internal geometries favoring a more efficient flow-transfer mechanisms.

Finally, in the three I-T curves examined (Fig. 8) a lower limit of mean rainfall intensity (approximately 1 $mm{\cdot}h^{-1}$) is established, below which there is no noticeable hydrodynamic responses in the springs. Consequently, small rainfall intensities do not have enough potential to saturate the water storage capacity of the soil-epikarst, so these rainfall events do not provoke significant risings in the flow rate of the discharge points.

In binary karst systems, such as it has been exemplified in this work, the contribution of diffuse and concentrated recharge largely governs the aquifer behavior. However, the input/output time-lag is far from being a feature driven entirely by the hydrogeological characteristics of the aquifer or recharge modalities. Although the development of the karst drainage network largely determines the velocity and capacity of water migration within the aquifer, several factors inherent to precipitation characteristics (intensity, rainfall amount, etc.) and to recharge mechanisms (saturation state in soil and epikarst, surface runoff, diffuse vs concentrated recharge, etc.) may operate as relevant modulators of response times. Moreover, the aquifer response to a single recharge event may be locally conditioned by other factors related to the remarkable anisotropy of karst media, such as the impact of hydrogeological barriers, interference among several preferential flow paths or siphonage phenomena). In all these cases, the cross-checking and application of statistical approaches with results derived from hydrochemistry and environmental isotopes (Trček, 2007; Houillion et al., 2016; Gil-Márquez et al., 2019), dye tracer test (Benischke et al., 2007; Goldshaider et al., 2008; Mudarra et al., 2014), or hydrochemical modelling, etc. (Maloszewski et al., 1992; Barberá et al., 2018; Mudarra

et al., 2019) help to quantify the complex recharge behavior of karst aquifers.

In current research, dye tracer tests permit to characterize several characteristics of groundwater flows regarding the preferential infiltration modality, which prevailing during the more intense recharge events. The global response time determined in the monitored springs (Fig. 8) is the sum of the diffuse and the concentrated recharge modalities. In this sense, plotting of time lag data versus precipitation intensity (I-T curve) has the potential to provide specific quantitative information on the impact of recharge modalities in flow dynamics of the aquifer as a whole. Likewise, the projection of the time lag times (T_{mc}) corresponding to the tracer tests on the I-T curve allows inferring the existence of hydraulic constraints that operate on the preferential flow paths defined by these tracer tests. Following all these insights, the establishment of the empirical relationship between the recharge impulses and their effects in the springs hydrodynamic constitutes a useful tool to predict potential affections to groundwater, with practicality implications in water resources management (Fig. 10). This is particularly relevant at the test site, when the rapid arrival of pollutants from livestock or anthropogenic pollution over recharge zones impacts on discharge points (Marín et al., 2021; Hartmann et al., 2021).

Nevertheless, additional information derived from subsequent dye tracer tests would be required to contrast results and make it possible to expand the set of connections between the preferential infiltration points and the outlets and, thus, characterize the specific response times (conditioned in turn by the water transmission capacity of the karst network) for the different drainage routes. The mapping of preferential drainage routes may contribute to characterize the functioning of the aquifer in terms of response times, a critical issue for resource management and risk mitigation in terms of human supply (Fig. 10).

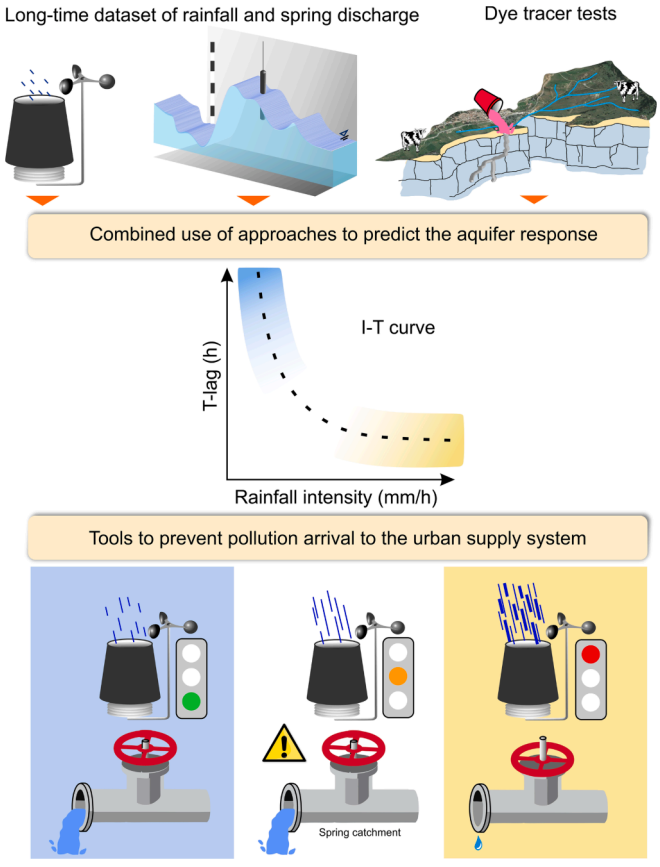

Fig. 10. Schematic illustration of the integrated approach applied in this study to predict potential affections to groundwater in karst aquifers, with usefulness implications in water resources management.

Moreover, the representativeness of the I-T curves is strongly conditioned by the reference meteorological station's location. The expansion of observatories network used to characterize the input signal can provide a more accurate information, both temporally and spatially, related to recharge events. Likewise, monitoring of concentrated inflows generated in the small catchment basins that inlet into the aquifer thought swallow holes can provide quantitative information about the magnitude of concentrated recharge and its role in the global aquifer response.

5. Conclusions

Detailed analysis of the response time to rainfall of several discharge points (springs) in a karst aquifer has revealed rainfall intensity as the major driver of the input signal transmission velocity. The combination of statistical approaches (CCF and SWCCF analysis) supported by direct measurements (Single events determinations of time-lag) has allowed characterizing a specific function (I-T curve) explaining the global response of each of the aquifer sectors in which a binary karst aquifer is segmented. The analysis can provide information on the expected response time of the springs to a rainfall event of a specific intensity, as well as drawing conclusions regarding the development and sectorial differences in the karst drainage network.

On the other hand, the differences observed among the response times obtained by means of dye tracer tests and the I-T curve can provide conclusive evidences regarding the presence of geometrical factors (aquifer structure, drainage network anisotropy) that may distort the global response of the system in the preferential drainage pathways. This research shows how the joint use of statistical analysis and experimental determinations in terms of response time can provide conclusive insights into the functioning and spatial distribution of the drainage network under different hydroclimatic conditions, which reduces uncertainties derived from the use of each technique separately.

The establishment of the springs global response time and the specific time lag between concentrated recharge processes and their impact on the discharge regime constitutes a useful and reliable tool for resource management and the planning and mitigation of risks generated by quick pollution events related to concentrated recharge mechanisms. These considerations may be relevant for the implementation of early warning systems (EWS) in those points destined for human supply, which requires a solid conceptual framework that provides the predictability of risk events, whose effectiveness is dependent on the anticipation with which the EWS can operate.

Fundings

This research was supported by the European Project "Karst Aquifer Resources availability and quality in the Mediterranean Area (KARMA)" PRIMA, ANR-18-PRIM-0005. The associated project PCI2019-103675 was funded by the Spanish Research Agency through the scientific program "Programación Conjunta Internacional". Additionally, it contributes to the project PID2019-111759RB-I00 supported by the Agencia Estatal de Investigación (AEI/https://doi.org/10.13039/501100011033) of the Spanish Government. Funding for open access charge: University of Malaga / CBUA.

CRediT authorship contribution statement

J.F. Martín-Rodríguez: Conceptualization, Methodology, Formal analysis, Investigation, Data curation, Writing – original draft, Writing – review & editing. **M. Mudarra:** Conceptualization, Methodology, Formal analysis, Investigation, Writing – review & editing, Supervision. **B. De la Torre:** Conceptualization, Writing – review & editing. **B. Andreo:** Conceptualization, Investigation, Resources, Writing – review & editing, Supervision, Project administration, Funding acquisition.

Declaration of Competing Interest

The authors declare that they have no known competing financial interests or personal relationships that could have appeared to influence the work reported in this paper.

Data availability

Data will be made available on request.

Acknowledgment

We thank to two anonymous reviewers who contributed to improving the original version of the manuscript, as well as to Corrado Corradini as Editor of Journal of Hydrology. We sincerely thank J.A. Barberá, J.M. Gil-Márquez, J. Martín, J. Prieto, J.M. Nieto, A.L. Morales and M.J. Civantos for their kind and selfless support in the field or laboratory works. This paper is a contribution of the Research Group RNM-308 of the Junta de Andalucía.

References

Andreo, B., Vías, J.M., Durán, J.J., Jiménez, P., López-Geta, J.A., Carrasco, F., 2008. Methodology for groundwater recharge assessment in carbonate aquifers: application to pilot sites in southern Spain. Hydrgeol. J. 16, 911–925. https://doi.org/10.1007/s10040-008-0274-5.

Andreo, B., Sánchez, D., Martín-Algarra, A., 2014. Hydrogeological Characterization and Water Resources Evaluation of Sierra de Grazalema Aquifers (Cádiz) for a Potential Implementation as Strategic Reserve in the Guadalete-Barbate River Water Basin [in Spanish]. Andalusian Water Agency Technical Report.

Bailly-Comte, B., Jourde, H., Pistre, S., 2009. Conceptualization and classification of groundwater-surface water hydrodynamic interactions in karst watersheds: Case of the karst watershed of the Coulazou River (Southern France). J. Hydrol. 376, 456–462. https://doi.org/10.1016/j.jhydrol.2009.07.053.

Bakalowicz, M., 2005. Karst groundwater: a challenge for new resources. Hydrgeol. J. 13 (1), 148–160.

Barberá, J.A., Mudarra, M., Andreo, B., De la Torre, B., 2018. Regional-scale analysis of karst underground flow deduced from tracing experiments: examples from carbonate aquifers in Malaga province, southern Spain. Hydrogeol J, 26:23-40. https://doi.org/10.1007/s10040-017-1638-5.

Benischke, R., Goldscheider, N., Smart, C., 2007. Tracer techniques. In: Goldscheider, N., Drew, D. (Eds.), Methods in karst hydrogeology. Taylor and Francis, London, pp. 147–170.

Bicalho, C., Batiot-Guilhe, J.L., Seidel, S., Van Exter, S., Jourde, H., 2012. Geochemical evidence of water source characterization and hydrodynamic responses in a karst aquifer. J. Hydrol. 450–451, 206–218. https://doi.org/10.1016/j.jhydrol.2012.04.059.

Bodin, J., Porel, G., Nauleau, B., Paquet, D., 2022. Delineation of discrete conduit networks in karst aquifers via combined analysis of tracer tests and geophysical data. Hydrol. Earth Syst. Sci. 26, 1713–1726. https://doi.org/10.5194/hess-26-1713-2022.

Charlier, J.B., Bertrand, C., Mudry, J., 2012. Conceptual Hydrogeological Model of Flow and Transport of Dissolved Organic Carbon in a Small Jura Karst System. J. Hydrol. 460–461, 52–64. https://doi.org/10.1016/j.jhydrol.2012.06.043.

De la Torre, B., Mudarra, M., Andreo, B., 2020. Investigating karst aquifers in tectonically complex alpine areas coupling geological and hydrogeological methods. J. Hydrol. X 6, 100047.

Delannoy, J.J., 1987. Inventaire bio-gèographique des espaces naturels d́Anadalousie: La Serranía de Grazalema et la Sierra de las Nieves. Casa de Velázquez-Agencia de Medio Ambiente de la Junta de Andalucía, 50pp.

Delannoy, J.J., 1999. Contribución al conocimiento de los macizos kársticos de las serranías de Grazalema y de Ronda. Karst en Andalucía. Eds: Durán, J.J., López-Martínez, J., 93-129.

Delbart, C., Valdes, D., Barbecot, F., Tognelli, A., Richon, P., Couchoux, L., 2014. Temporal variability of karst aquifer response time established by the sliding-windows cross-correlation method. J. Hydrol. 511, 580–588.

Doerfliger, N., Zwahlen, F., 1998. Practical guide, groundwater vulnerability mapping in karstic regions (EPIK). Swiss Agency for the Environment, Forests and Landscape. Bern, Switzerland, p. 56.

El-Hakim, M., Bakalowicz, M., 2007. Significance and origin of very large regulating power of some karst aquifers in the Middle East. Implication on karst aquifer classification. J. Hydrol. 333, 329–339. https://doi.org/10.1016/j.jhydrol.2006.09.003.

EU, 1995. Hydrogeological aspects of groundwater protection in karstic areas, Final report (COST action 65). European Commission, Directorat-General XII Science, Research and Development, Report EUR 16547. Brussels, Luxemburg. 446pp.

Fiorillo, F., Doglioni, A., 2010. The relation between karst spring discharge and rainfall by cross-correlation analysis (Campania, southern Italy). Hydrgeol. J. 18 (8), 1881–1895.

Ford, D.C., Williams, P.W., 2007. Karst Hydrogeology and Geomorphology. Wiley, Chichester, United Kingdom, p. 562.

Fu, Z.Y., Chen, H.S., Zhang, W., Xu, Q.X., Wang, S., Wang, K.L., 2015. Subsurface flow in a soil-mantled subtropical dolomite karst slope: A field rainfall simulation study. Geomorphology 250, 1–114. https://doi.org/10.1016/j.geomorph.2015.08.012.

Galibert, P.Y., 2016. Quantitative estimation of water storage and residence time in the epikarst with time-lapse refraction seismic. Geophys. Prospect. 64 (2), 431–444. https://doi.org/10.1111/1365-2478.12272.

Gil-Márquez, J.M., Andreo, B., Mudarra, M., 2019. Combining hydrodynamics, hydrochemistry, and environmental isotopes to understand the hydrogeological functioning of evaporite-karst springs. An example from southern Spain. J. Hydrol. 576, 299–314. https://doi.org/10.1016/j.jhydrol.2019.06.055.

Goldscheider, N., 2005. Fold structure and underground drainage pattern in the alpine karst system Hochifen-Gottesacker. Eclogae Geol. Helv. 98, 1–17. https://doi.org/10.1007/s00015-005-1143-z.

Goldscheider, N., Meiman, J., Pronk, M., Smart, C., 2008. Tracer test in karst hydrogeology and speleology. Int. J. Speleol. 37 (1), 27–40. https://doi.org/10.5038/1827-806X.37.1.3.

Groves, C., 2007. The geological and geomorphological framework. In: Goldscheider, N., Drew, D. (Eds.), Methods in karst hydrogeology. International Contribution to Hydrogeology, IAH, vol 26. Taylor and Francis/Balkema, London, pp. 9–23.

Hartmann, A., Jasechko, S., Gleeson, T., Wada, Y., Andreo, B., Barberá, J.A., Brielmann, H., Bouchaou, L., Charlier, J.B., Darling, W.G., Filippini, M., Garvelmann, J., Goldscheider, N., Kralik, M., Kunstmann, H., Ladouche, B., Lange, J., Lucianetti, G., Martín, J.F., Mudarra, M., Sánchez, D., Stumpp, C., Zagana, E., Wagener, T., 2021. Risk of groundwater contamination widely underestimated because of fast flow into aquifers. Proc Natl Acad Sci (PNAS), 118(20):e2024492118. .

Jiang, G.H., Guo, F., Wu, J.C., Li, H.J., Sun, H.L., 2008. The threshold value of epikarst runoff in forest karst mountain area. Environ Geo 55 (1), 87–93. https://doi.org/10.1007/s00254-007-0967-4.

Jiménez-Bonilla, A., Expósito, I., Balanyá, J.C., Díaz-Azpiroz, M., 2017. Strain partitioning and relief segmentation in arcuate fold and-thrust belts: a case study from the western Betics. J. Iber. Geol. 43 (3), 497–518.

Jukić, D., Denić -Jukić, V., 2011. Partial spectral analysis of hydrological time series. J. Hydrol. 400 (1–2), 223–233. https://doi.org/10.1016/j.jhydrol.2011.01.044.

Jukić, D., Denić -Jukić, V.,, 2015. Investigating relationships between rainfall and karst-spring discharge by higher-order partial correlation functions. J. Hydrol. 530, 24–36. https://doi.org/10.1016/j.jhydrol.2015.09.045.

Käss, W., 1998. Tracing technique in geohydrology. Balkema, Brookfield, MA, p. 581.

Konapala, G., Mishra, A.K., Wada, Y., Mann, M.E., 2020. Climate change will affect global water availability through compounding changes in seasonal precipitation and evaporation. Nat. Commun. 11 (1), 3044. https://doi.org/10.1038/s41467-020-16757-w.

Larocque, M., Mangin, A., Razack, M., Banton, O., 1998. Contribution of correlation and spectral analyses to the regional study of a large karst aquifer (Charente, France). J. Hydrol. 205 (3-4), 217–231.

Lee, L.J.E., Lawrence, D.S.L., Price, M., 2006. Analysis of water-level response to rainfall and implications for recharge pathways in the Chalk aquifer, SE England. J. Hydrol. 330, 604–620. https://doi.org/10.1016/j.jhydrol.2006.04.025.

Lorette, G., Lastennet, R., Peyraube, N., Denis, A., 2018. Groundwater-flow characterization in a multilayered karst aquifer on the edge of a sedimentary basin in western France. J. Hydrol. 566, 137–149. https://doi.org/10.1016/j.jhydrol.2018.09.017.

Maloszewski, P., Benischke, R., Harum, T., 1992. Mathematical modelling of tracer experiments in the karst of Lurbach-System. Steir Beitr Z Hydrogeologie 43, 116–136.

Mangin, A., 1981. Utilisation des analyses correlatoire et spectrale dans l'approche des systèmes hydrologiques. Computers Rendues Acad Sci Paris 293 (401), 404.

Mangin, A., 1984. Pour une meilleure connaissance des systemes hydrologiques a partir des analyses correlatoire et spectrale. J. Hydrol. 67, 25–43.

Marín, A.I., Andreo, B., 2015. Vulnerability to contamination of karst aquifers. In: Stevanović Z (eds) Karst aquifers: characterization and engineering. In: Professional practice in earth sciences. Springer, Cham, Switzerland, 251-266.

Marín, A.I., Martín-Rodríguez, J.F., Barberá, J.A., Fernández-Ortega, J., Mudarra, M., Sánchez, D., Andreo, B., 2021. Groundwater vulnerability to pollution in karst aquifers, considering key challenges and considerations: application to the Ubrique springs in southern Spain. Hydrogeol J, 29:379-396 https://doi.org/10.1007/s10040-020-02279-8.

Martín-Algarra, A., 1987. Evolución geológica alpina del contacto entre las Zonas Internas y las Externas de la Cordillera Bética. University of Granada (Spain), p. 1171 pp.. PhD Thesis.

Martín-Rodríguez, J.F., Mudarra, M., Andreo, B., De la Torre, B., 2022. Combining quantitative analysis tools (cross-correlation analysis and dye tracer test) to asses response times in karst aquifers. The Ubrique karst system (southern Spain). In: Andreo, B., Barberá, J.A., Durán-Valsero, J.J., Gil-Márquez, J.M., Mudarra, M. (Eds.), Eurokarst 2022. Advances in the Hydrogeology of karst and Carbonate Reservoirs. Springer, Switzerland, pp. 41–47. https://doi.org/10.1007/978-3-031-16879-6_7.

Mudarra, M., Andreo, B., Barberá, J.A., Mudry, J., 2014. Hydrochemical dynamics of TOC and NO^{3-} contents as natural tracers of infiltration in karst aquifers. Environ. Earth Sci. 71 (2), 507–523. https://doi.org/10.1007/s12665-013-2593-7.

Mudarra, M., Hartmann, A., Andreo, B., 2019. Combining experimental methods and modeling to quantify the complex recharge behavior of karst aquifers. Water Resour. Res. 55, 1384–1404. https://doi.org/10.1029/2017WR021819.

Padilla, A., Pulido-Bosch, A., 1995. Study of hydrographs of karstic aquifers by means of correlation and cross-spectral analysis. J. Hydrol. 168 (1-4), 73–89.

Panagopoulos, G., Lambrakis, N., 2006. The contribution of time series analysis to the study of the hydrodynamic characteristics of the karst systems: application on two typical karst aquifers of Greece (Trifilia, Almyros Crete). J. Hydrol. 329 (3-4), 368–376.

Perrin, J., Luetscher, M., 2008. Inference of the structure of karst conduits using quantitative tracer tests and geological information: example of the Swiss Jura. Hydrogeol J, 16 (5): 951–967.

Perrin, J., Jeannin, P.Y., Zwahlen, F., 2003. Epikarst Storage in a Karst Aquifer: A Conceptual Model Based on Isotopic Data. Milandre Test Site, Switzerland, J Hydrol 279, 106–124. https://doi.org/10.1016/S0022-1694(03)00171-9.

Richts, A., Vrba, J., 2017. Groundwater resources and hydroclimatic extremes: mapping global groundwater vulnerability to floods and droughts. Environ Earth Sci, 75:926 https://doi.org/10.1007/s12665-016-5632-3.

Sánchez, D., Antonio Barberá, J., Mudarra, M., Andreo, B., Martín, J.F., 2018. Hydrochemical and isotopic characterization of carbonate aquifers under natural flow conditions, Sierra Grazalema Natural Park, southern Spain. SP 466 (1), 275–293.

Sánchez, D., Martín-Rodríguez, J.F., Mudarra, M., Andreo, B., López-Rodríguez, M., Navas, M.R., 2016. Time lag analysis of natural responses during unitary recharge events to assess the functioning of carbonate aquifers in Sierra de Grazalema Natural Park (southern Spain). In: Renard, P., Bertrand, C. (eds) EuroKarst 2016. Advances in Karst Science. Springer, Berlin, 157–167. DOI: 10.1007/978-3-319-45465-8_16.

Sanz de Galdeano, C., Prieto-Mera, J., Andreo, B., 2019. Structure of the Alpujarride Complex and hydrogeological observations to the NW of Sierra Tejeda (Granada and Malaga provinces, Betic Internal Zone, Spain). Estud. Geol. 75 (1), e090.

Schuler, P., Stoecki, L., Schnegg, P.-A., Bunce, C., Gill, L., 2020. A combined-method approach to trace submarine groundwater discharge from a coastal karst aquifer in Ireland. Hydrogeol J, 28:561–577. https://doi.org/10.1007/s10040-019-02082-0.

Stevanović, Z., 2018. Global distribution and use of water from karst aquifers. Geol. Soc. Lond. Spec. Publ. 466 (1), 217. https://doi.org/10.1144/SP466.17.

Trček, B., 2007. Flow and solute transport monitoring in the karst aquifer in SW Slovenia. Environ. Geol. 55 (2), 269–276. https://doi.org/10.1007/s00254-007-1001-6.

Worthington, S., Ford, D., 2009. Self-organized permeability in carbonate aquifers. Ground Water 47, 326–336.